Dalton Transactions

PAPER

View Article Online
View Journal | View Issue

Cite this: *Dalton Trans.*, 2016, **45**, 8637

Ambient pressure synthesis of MIL-100(Fe) MOF from homogeneous solution using a redox pathway†

Felix Jeremias,[a,b] Stefan K. Henninger*[a] and Christoph Janiak*[b]

Received 26th March 2016,
Accepted 24th April 2016

DOI: 10.1039/c6dt01179a

www.rsc.org/dalton

Micro- to mesoporous iron(III) trimesate MIL-100(Fe) is a MOF of high interest for numerous applications. With regard to large-scale synthesis, *e.g.*, by continuous flow or the *in situ* deposition of coatings, a replacement for the conventional, hydrothermal low-yield fluoride-containing synthesis is desirable. In this contribution, we present a method to synthesize crystalline fluoride-free MIL-100(Fe) from iron(III) nitrate and trimesic acid in zeotropic DMSO/water solution at normal ambient pressure involving a DMSO–nitrate redox pathway. Yields of 72%, surface areas of S_{BET} = 1791 m^2 g^{-1} and pore volumes of V_{pore} = 0.82 cm^3 g^{-1} were achieved.

Introduction

Metal–organic frameworks (MOFs) are the subject of ongoing attention[1,2] due to their high porosity which promises applications in, *e.g.*, gas storage,[3] gas[4,5] and pollutant[6] separation processes, drug delivery,[7] heterogeneous catalysis,[8,9] heat transformation[10,11–13] *etc.*[14]

Among the about 20 000 MOFs known to date, the class of MIL compounds (MIL = Materials of Institute Lavoisier), which was pioneered by Férey and his group,[5,16] sticks out due to their higher hydrothermal stability compared to many of the other MOFs.[17]

Further, among the abundancy of known MIL-MOF structures, mesoporous MIL-100 has received special attention in the literature with respect *e.g.* to its catalytic, gas separation, gas storage, drug delivery[7] and water sorption properties.[2,11,18–20] MIL-100(M) compounds are three-dimensional chromium(III), iron(III) or aluminium(III) benzene-1,3,5-tricarboxylates of formula 3D-$[M_3(\mu\text{-}O)(X)(H_2O)_2(btc)_2{\cdot}nH_2O]_n$, (M = Cr,[21,22] Fe,[18,23] Mn,[24] V[25] or Al,[26] X = OH, F, btc = benzene-1,3,5-tricarboxylate, trimesate). The porosity of MIL-100 originates from both 25 Å and 29 Å mesopores accessible *via* 5.5 Å and 8.6 Å windows, respectively (Fig. 1).[18] MIL-100(Cr, Fe) have been proven to be hydrothermally very stable MOFs, even with regard to repeated adsorption/desorption cycles using water vapor.[11,22] In particular, MIL-100(Fe) can be prepared from toxicologically and environmentally benign building blocks,[27] – except for the use of HF required by the original synthesis procedure[18] – with cost-efficient components. Despite these advantages, crystalline MIL-100(Fe) is still not commercially available. This can be attributed to the fact that its syntheses must be carried out in water, mostly at T > 100 °C, starting from a heterogeneous reaction mixture containing iron(III) chloride and trimesic acid or its trimethyl ester.[18,20,28–30] The original synthesis procedure for MIL-100(Fe) was developed by Férey *et al.*[18] In this original procedure, hydrofluoric acid, HF was used in strongly acidic solution (pH < 1, HNO_3). The use of HF (a classified chemical toxicant) or acidic fluoride solutions is not desirable for large-scale or commercial syntheses.[31] More important, overpressure and/or heterogeneous reaction mixtures render reaction control difficult and require expensive equipment, especially when it comes to scale-up. Continuous-flow synthesis has successfully

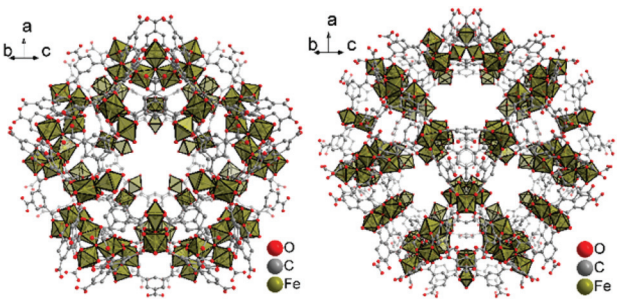

Fig. 1 Small S cage (left) and large L cage (right) in MIL-100(Fe). Objects are not drawn to scale. Hydrogen atoms and solvent molecules of crystallization are not shown. Graphics produced by Diamond[15] from cif-file for MIL-100(Fe) (CSD-Refcode CIGXIA, CCDC no. 640536).[1]

[a]*Department of Thermally Active Materials and Solar Cooling, Fraunhofer Institute for Solar Energy Systems (ISE), Heidenhofstr. 2, D-79110 Freiburg, Germany. E-mail: stefan.henninger@ise.fraunhofer.de*
[b]*Institut für Anorganische Chemie und Strukturchemie, Universität Düsseldorf, Universitätsstr. 1, D-40225 Düsseldorf, Germany. E-mail: janiak@uni-duesseldorf.de*
†Electronic supplementary information (ESI) available: PXRD of $Fe(NO_3)_3{\cdot}6DMSO$, dew point/bubble point curves of DMSO/water. See DOI: 10.1039/c6dt01179a

been implemented for several MOFs as a promising method to their economic production.[32] It can be expected that the space-time yield of a continuous process will exceed that of any batch process by far. However, in the case of MIL-100(Fe), the present demand for hydrothermal reaction conditions increases the technical complexity. Sub-hydrothermal reaction conditions, on the other hand, are known to lead to clogging.[33] *In situ* procedures, *e.g.*, for the fabrication of coatings[12,13] are also much more complicated to realize with the present hydrothermal procedures for MIL-100(Fe), be it with the addition of HF or without. Part of the commercial success of MOFs depends on the development of improved synthesis procedures.[34] Recently, we reported a high-yield, fluoride-free and large-scale synthesis of related MIL-101(Cr).[35]

This contribution investigates the approach to overcome the overpressure and HF issue in replacing part of the water in the reaction mixture by a high-boiling, polar solvent forming a zeotropic mixture. This mixture should dissolve all starting materials and keep liquid water in the reaction-mixture even at $T > 100$ °C. Dimethyl sulfoxide, DMSO, $(CH_3)_2S{=}O$ is an environmentally benign, aprotic and highly polar solvent forming zeotropic mixtures with water.[36] In this contribution, we demonstrate the successful fabrication of MIL-100(Fe) from a homogeneous, fluoride-free solution at ambient pressure from a solvent where unreacted trimesic acid remains in solution.

Experimental section

Note on DMSO

Dimethyl sulfoxide is less harmful than any other highly polar, aprotic, organic solvent. DMSO is a solvent with a median lethal dose higher than ethanol. DMSO is not listed as toxic or especially harmful. At high temperatures, it is flammable, and when brought into contact with skin, irritations may occur. DMSO is even used as an ingredient for pharmaceutical formulations (ointments). In medicine, DMSO is predominantly used as a topical analgesic, a vehicle for topical application of pharmaceuticals, as an anti-inflammatory, and an antioxidant substance.

General synthesis

In a 250 mL three-necked round bottom flask equipped with a magnetic stirring bar, a reflux condenser and an internal thermometer, 1.12 g (5.3 mmol) of trimesic acid (≥98%, TCI) were dissolved in 40 mL of dimethyl sulfoxide. Solutions of 8 mmol (referred to Fe^{3+}) of iron(III) nitrate, chloride, mesylate, hydrogen sulfate or sulfate in 8 mL of deionized water were prepared as described in the ESI.† The pH value was set according to Scheme 1 using the corresponding acids.

Before merging the metal salt solution and the trimesic acid solution, the latter was heated to a temperature of 90 °C in order to avoid precipitation of $[Fe(DMSO)_6](NO_3)_3$ (see ESI with Fig. S1†), upon addition of iron(III) nitrate into the DMSO

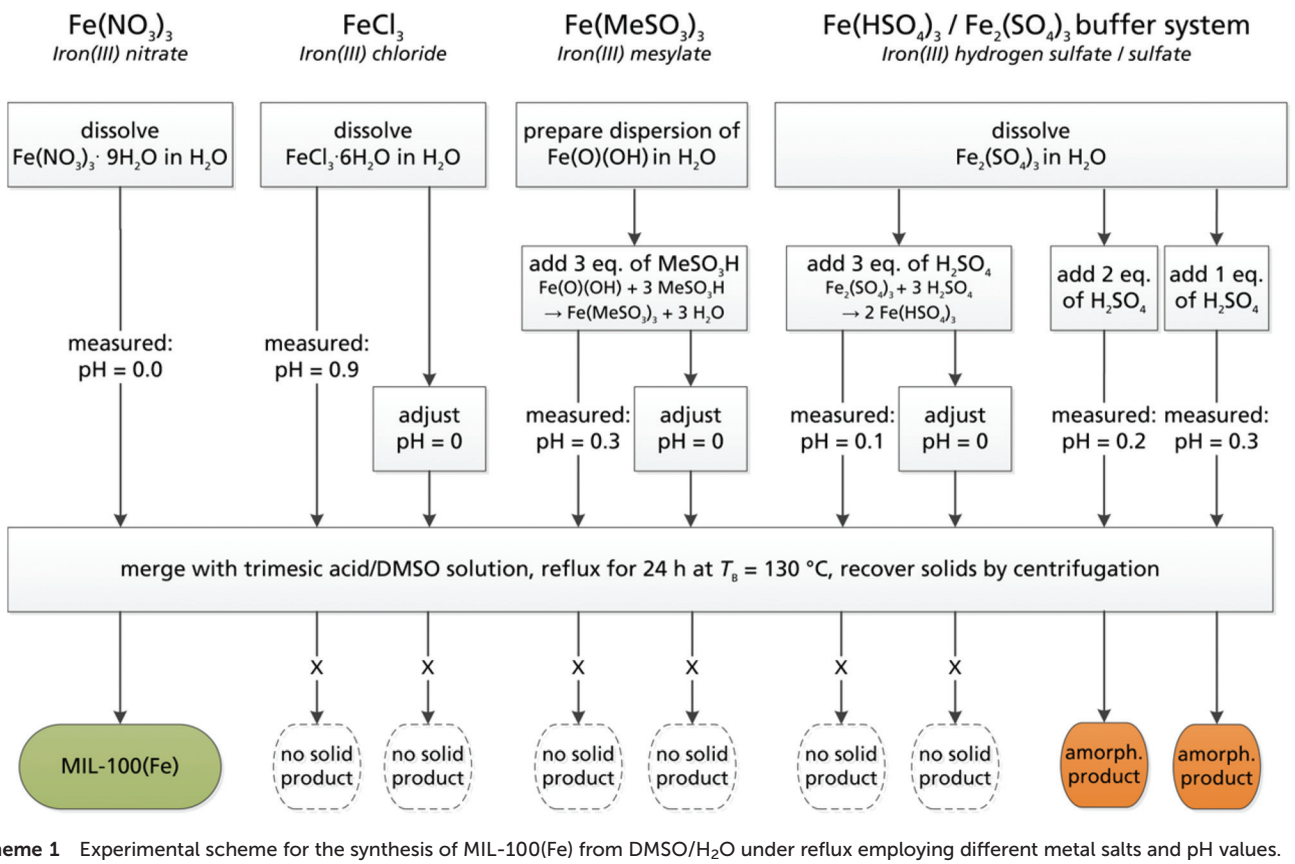

Scheme 1 Experimental scheme for the synthesis of MIL-100(Fe) from DMSO/H_2O under reflux employing different metal salts and pH values.

solution of trimesic acid. Solid $[Fe(DMSO)_6](NO_3)_3$ is a potential explosive but can be handled in the solution state.[37] After merging, the clear, yellow mixture was heated further to its boiling point of 130 °C with gentle stirring. Within 30 min, the yellow-green, clear solution turned amber and then turbid when iron(III) nitrate was used. The solid product was separated by centrifugation of the still warm solution (80 °C) after 24 h.

Influence of reaction time

The synthesis was performed as stated above. The precipitate was retrieved at set times (see Table 1) by centrifugation of the hot solution and the clear solution was continued to reflux.

Influence of HNO_3 addition

The influence of additional HNO_3 on the synthesis was investigated by adding 0, 0.5, 1 or 2 HNO_3 equivalents with respect to Fe (8 mmol).

Activation

Activation was performed by stirring the solid, as synthesized MIL-100(Fe) product thrice in 25 mL each of a mixture of DMSO/H_2O = 4 : 1 (v/v) for 1 h, 1 h and 24 h. Then, the solid product was stirred thrice in 25 mL each of ethanol for 1 h, 1 h and 24 h, and air-dried for 12 h at 80 °C. The washing solutions were separated by centrifugation and discarded. Yield: 1.25 g for the 24 h reflux synthesis using iron(III) nitrate (72%). Other yields are given in Tables 1 and 2.

Analytical methods

Powder X-ray diffractograms were acquired on a Bruker® D8 Advance with DaVinci® design using Cu-Kα radiation, a Lynxeye detector, 0.02° and 1 s per step. Diffractograms were obtained on flat layer sample holders which led to the low relative intensities measured at low 2-theta angles (<5°) compared to the simulated pattern. Nitrogen adsorption isotherms were obtained at 77 K on a Quantachrome® Nova, after degassing for 24 h in fine vacuum at 120 °C.

Table 1 Time-dependent product yields and porosity data for activated MIL-100(Fe) samples synthesized from iron(III) nitrate and trimesic acid in the DMSO water system

Sample	Retrieved after	Yield, activated (mg)	S_{BET} [a] ($m^2\ g^{-1}$)	V_{pore} [b] ($cm^3\ g^{-1}$)
1	24 h	1250	1215	0.61
2a	2 h	115	1024	0.62
2b	4 h	109	1405	0.71
2c	8 h	147	1513	0.73
2d	24 h	286	1507	0.72
2e	48 h	No further precipitation observed		

[a] Calculated in the pressure range $0.05 < p/p_0 < 0.2$ from N_2 sorption isotherm at 77 K with an estimated standard deviation of ±50 $m^2\ g^{-1}$. [b] Calculated from N_2 sorption isotherm at 77 K (p/p_0 = 0.95) for pores ≤20 nm.

Table 2 Surface area and pore volume for MIL-100(Fe) with various equivalents of HNO_3 as additive

HNO_3 equivalents to Fe[a]	Initial HNO_3 conc.[b] ($mol\ L^{-1}$)	S_{BET} [c] ($m^2\ g^{-1}$)	V_{pore} [d] ($cm^3\ g^{-1}$)
0	0	1412	0.71
0.5	0.083	1539	0.73
1	0.17	1791	0.82
2	0.33	1058	0.49

[a] Molar ratio HNO_3 to Fe. The Fe : H_3btc ratio is always 3 : 2. [b] Calculated from the amount of added HNO_3 and the volume of the reaction solution. [c] Calculated in the pressure range $0.05 < p/p_0 < 0.2$ from N_2 sorption isotherm at 77 K with an estimated standard deviation of ±50 $m^2\ g^{-1}$. [d] Calculated from N_2 sorption isotherm at 77 K (p/p_0 = 0.95) for pores ≤20 nm.

Results and discussion

Synthesis of MIL-100(Fe) under reflux conditions in DMSO/water solution using different metal salts

A mixture of DMSO : water = 4 : 1 (v : v) was selected as the solvent due to its ability to dissolve the starting materials already at room temperature, and because of the possible high water content. Furthermore, this mixture has an ambient pressure (101.3 kPa) boiling point of 130 °C (Fig. S2, ESI†). This boiling point matches the temperature given in a common hydrothermal procedure yielding highly porous MIL-100(Fe) without addition of HF.[28,36] Iron(III) nitrate, chloride, mesylate and a sulfate/hydrogen sulfate system ($pK_a(HSO_4^-)$ = 1.9) were examined as Fe(III) sources with different anions. Metal salt precursors were selected according to the criteria of solubility in water/DMSO mixtures, the fact that MOFs have been successfully prepared using chloride, nitrate, sulfate anions and low (nitrate, sulfate, mesylate) anion coordination strength towards Fe^{3+}. In order to find the optimal synthesis conditions for MIL-100(Fe) at ambient pressure, not only the iron salt, but also the pH was varied systematically (see Scheme 1 for an overview): first, all the metal salt solutions were used as prepared. In a second run, the pH of the Fe hydrogen sulfate, chloride and mesylate solutions was set to pH = 0, which is the initial, direct pH value of the 1 mol L^{-1} iron(III) nitrate solution (without acid addition).

Regardless of the pH, a color change of the solution (yellow to red), followed by the precipitation of MIL-100(Fe) could be observed only when using the nitrate salt (see Scheme 1). This indicates the generation of the $Fe_3(\mu_3\text{-}O)$ cluster forming the secondary building unit of MIL-100(Fe).[38] At the same time, NO_x fumes were observed inside the reflux condenser.

The fluoride-free synthesis of MIL-100(Fe) in DMSO/water under ambient pressure yielded a product in good yield (72%) with a BET surface area of S_{BET} = 1215 $m^2\ g^{-1}$ and pore volume V_{pore} = 0.61 $cm^3\ g^{-1}$. This has to be compared with literature data for MIL-100(Fe) from hydrothermal synthesis with the addition of HF and S_{BET} = 1917 $m^2\ g^{-1}$, V_{pore} = 1.00 $cm^3\ g^{-1}$ (ref. 11) or $S_{Langmuir}$ > 2800(100) $m^2\ g^{-1}$.[18] Under hydrothermal conditions but without the addition of HF, S_{BET} = 1800 $m^2\ g^{-1}$,

and V_{pore} = 1.15 cm^3 g^{-1} were achieved.[29] From a reaction slurry containing trimesic acid, iron(III) nitrate and water, MIL-100 with S_{BET} = 1836 m^2 g^{-1} and V_{pore} = 1.1 cm^3 g^{-1} was said to be obtained at 95 °C.[20] The slightly lower porosity of MIL-100(Fe) produced by the DMSO/water approach can be attributed to the possible presence of an amorphous phase, as well as the overall slightly lower crystallinity of the product. Furthermore, the presence of hardly soluble dimethyl sulfone ($DMSO_2$) in the pores cannot be ruled out.

The successful action of HF in terms of improved crystallinity and porosity has been documented,[34,39] still its poisonous nature renders its replacement highly desirable even at the expense of slightly less surface area or pore volume.[35]

No solid products were obtained from the iron chloride, mesylate or hydrogen sulfate starting materials. From the hydrogen sulfate/sulfate system, only amorphous precipitates were formed, which we ascribe to the fact that the sulfate salt is the most basic among the investigated precursors, resulting in fast, non-crystalline precipitation.

Time-dependent MIL-100 formation

In order to investigate the influence of reaction time on the product formation, the precipitate was centrifuged off after fixed amounts of time, and the clear, red centrifugate was continued to reflux. The separated solids **2a** to **2d** were activated separately and it is apparent that both the crystallinity (Fig. 2) and the microporosity of the product increase with reaction time (although the formation rate does not). The sorption isotherms for **1** and **2a–2d** exhibit a very similar curvature with the typical inflection point at p/p_0 = 0.1, which is assigned to the two different cages (*cf.* Fig. 1). Surprisingly, the samples **2b**, **2c** and **2d** separated after 4 h, 8 h and 24 h reaction time, respectively, yield a significantly increased BET surface area and porosity compared to the 24 h direct-sample **1**. We explain

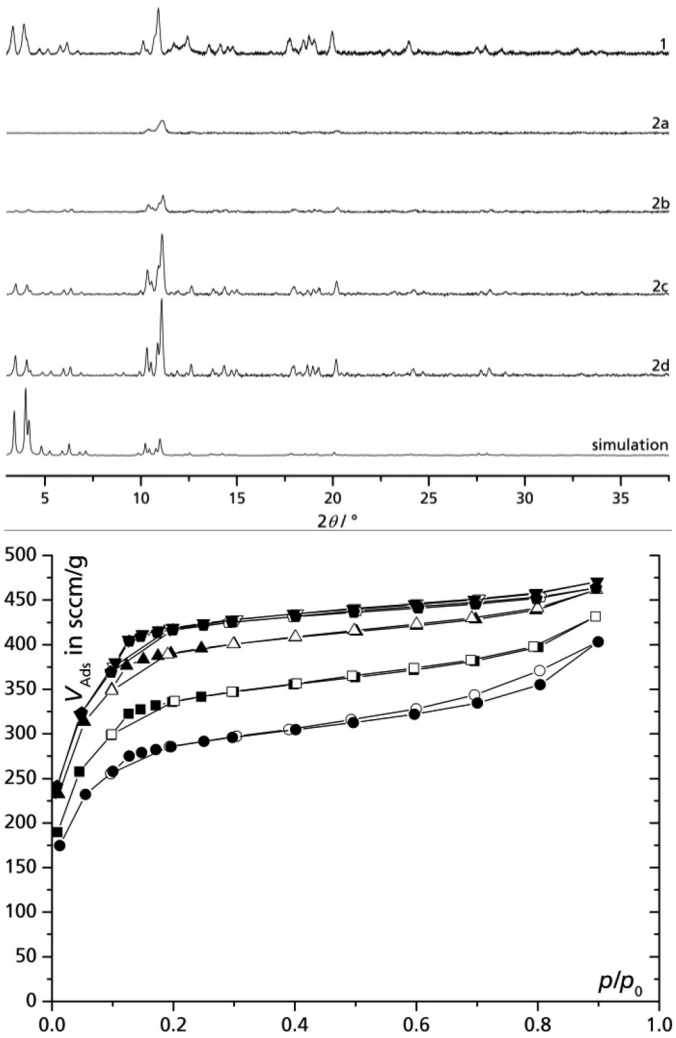

Fig. 2 Powder X-ray diffractograms (top) and nitrogen adsorption isotherms (77 K, bottom) of activated MIL-100(Fe) prepared by the DMSO/water route using iron(III) nitrate in a single batch with 24 h reaction time (**1**), and of products removed from the reaction solution by centrifugation after different reaction times (**2a–2d**): **1** – 24 h without interruption (■), **2a** – 2 h (●), **2b** – 4 h (▲); **2c** – 8 h (▼), **2d** – 24 h (⬟). Filled symbols = adsorption, empty symbols = desorption; see also Table 1).

the improved sample characteristics of **2b** to **2d** by a seeding effect of residual nano-MIL particles remaining in the "solution" after centrifugation. MIL nanoparticles of less than 0.2 μm can only be separated by high-speed ultracentrifugation.[9] These nano-seeds can then lead to improved crystallization from a solution which has become more dilute compared to the rapidly formed crystallites of **2a** from a more concentrated homogeneous solution. Sample **1** then presents an averaged BET surface area and porosity from rapidly precipitated low-quality product (*cf.* **2a**) and slower formed high-quality products (*cf.* **2b** to **2d**) when the solution has become more dilute – a drawback of this otherwise attractive fractionated crystallization or synthesis of MIL-100(Fe).

Influence of HNO_3 addition

It was recently shown in the fluoride-free synthesis of MIL-101(Cr) that an increased HNO_3 content (up to one equivalent *versus* Cr) in the reaction mixture could substantially improve the yield, BET surface area and pore volume.[35] In order to verify whether a higher initial content of nitric acid also improves the crystallization of MIL-100(Fe) syntheses 0, 0.5, 1 and 2 equivalents of nitric acid were added to the reaction mixture of iron(III) nitrate and trimesic acid in DMSO/water. The HNO_3 addition is based on the perception that acidification should shift the equilibrium away from the formation of MIL-100(Fe) as nitric acid is released during the process. All products are of good crystallinity (Fig. 3) but improvement of product quality, judged by porosity, could be reached compared to experiments without addition of nitric acid (Table 2). The concentration of HNO_3 determines the ligand deprotonation equilibrium in the reaction mixture and is therefore probably the key value rather than the ratio of HNO_3 to Fe. Yet, it is likely that the most efficient HNO_3 concentration will lie within the same order of magnitude as the Fe concentration, therefore, we gave and worked here with more illustrative HNO_3 to Fe equivalents. At 1 eq. of HNO_3 the highest BET surface area and pore volume was obtained (approaching the literature data from fluoride-containing syntheses, *vide supra*) which decreases considerably with higher amounts of HNO_3. This finding matches the recent observation on the HNO_3 effect in the synthesis of MIL-101(Cr). There, also the addition of 1.0 equivalent of nitric acid in synthesis produced the best porosity of MIL-101(Cr).

Mechanism of MIL-100 formation

To the best of our knowledge, MIL-100(Fe) has been synthesized up to date only using water as the solvent or dispersant. Under these conditions, formation of MIL-100(Fe) occurs most likely according to the general hydrothermal MOF formation mechanism: deprotonation of the linker due to increased temperature (Le Chatelier's principle) and withdrawal of the deprotonated linker from the equilibrium by precipitation, resulting in further deprotonation of the linker acid. Using the DMSO/water system, the formation mechanism appears to be fundamentally different:

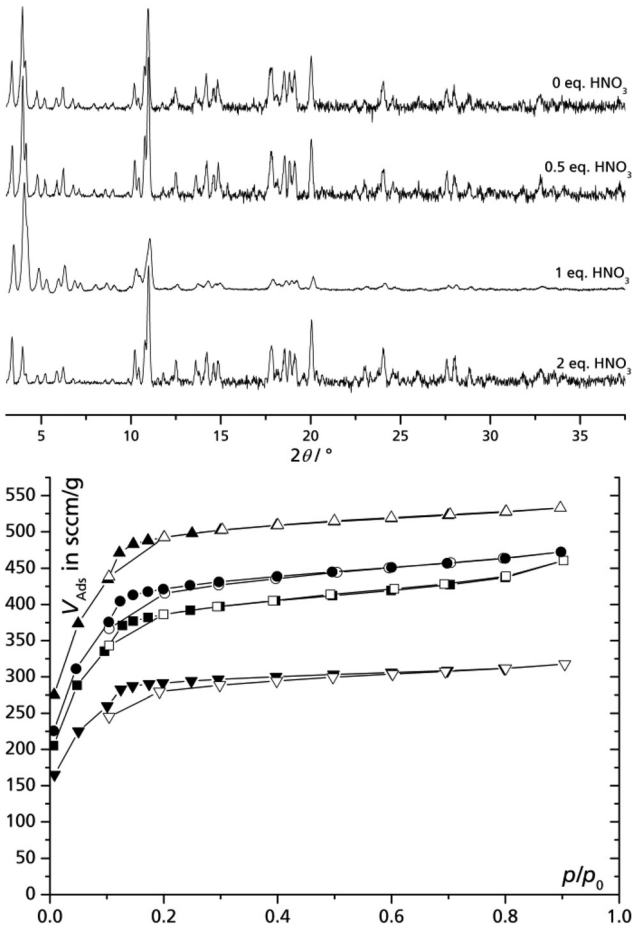

Fig. 3 Powder diffractograms (top) and nitrogen adsorption isotherms (77 K, bottom) of MIL-100(Fe) prepared from iron nitrate and trimesic acid using a DMSO water solution with different equivalents of nitric acid (relative to Fe) added. Cu-Kα radiation. ■ – 0 eq., ● – 0.5 eq., ▲ – 1 eq., ▼ – 2 eq. Filled symbols = adsorption, empty symbols = desorption; see also Table 2).

From the fact that MIL-100(Fe) is formed only when iron(III) nitrate is used as the Fe source, we deduce that there is a specific mechanism involved in the formation of MIL-100(Fe) in the DMSO/water solvent system. In DMSO/water there is an initial complexation of Fe^{3+} with formation of DMSO complexes $[Fe(DMSO)_{6-n}(H_2O/OH)_n]^{3+}$ instead of only aqua-hydroxido complexes, such as $[Fe(H_2O)_5(OH)]^{2+}$. Dimethyl sulfoxide is known to form strong complexes with Fe^{3+} cations. $[Fe(DMSO)_6](NO_3)_3$, where DMSO coordinates octahedrally to Fe^{3+} *via* the oxygen atom (Fig. S3, ESI†), precipitates from solutions of iron(III) nitrate in DMSO (see ESI†).[37,40] This has also been observed during our work when the solutions were allowed to sit at room temperature for longer than 5 min with no or too little water added, and the precipitate was hardly soluble in water. This insolubility is explained by the DMSO methyl groups forming the surface of the $[Fe(DMSO)_6]^{3+}$ cation and rendering it hydrophobic (Fig. S3, ESI†). Formation of Fe–DMSO complexes will occur with all iron salts used in Scheme 1 in DMSO solution. The special property of the

nitrate anion among the used iron salts (Scheme 1) is its redox property. DMSO is known to decompose partially under experimental conditions generating *e.g.* formaldehyde and dimethyl sulfide (DMS).[36] The distinct smell of DMS could be clearly noticed during all experiments. Especially DMS, but also DMSO reduces nitrate in an acidic environment converting it to nitrite (eqn (1) and (2)).[41]

$$NO_3^- + DMS \rightarrow NO_2^- + DMSO \quad (1)$$

$$NO_3^- + DMSO \rightarrow NO_2^- + DMSO_2 \quad (2)$$

Nitrite in acidic solution (nitric acid) decomposes easily under disproportionation (eqn (3)).

$$3NO_2^- + 2H^+ \rightarrow NO_3^- + 2NO + H_2O \quad (3)$$

Also formation of nitric oxide can occur either by a similar reductive pathway (eqn (4)) or by comproportionation of nitrate and nitrite (eqn (5)).[42] NO_x fumes were observed inside the reflux condenser.

$$2NO_3^- + DMS + 2H^+ \rightarrow 2NO_2 + DMSO + H_2O \quad (4)$$

$$NO_3^- + NO_2^- + 2H^+ \rightarrow 2NO_2 + H_2O \quad (5)$$

Reactions (3)–(5) all consume protons thereby slowly increasing the pH, as required for the formation of the trinuclear $\{Fe_3(\mu_3\text{-}O)(H_2O)_2(OH)\}$ secondary building unit with its oxido and hydroxido anions and for the deprotonation of trimesic acid. Thus, for the formation of MIL-100(Fe) upon heating of iron(III) nitrate (with trimesic acid) in DMSO/water a special chemoreductive pathway is involved.

Dincă *et al.* recently showed that the reduction of nitrate is also key to the formation of MOF-5 using an electroreductive synthesis.[43]

Conclusions and outlook

The investigations presented in this contribution provide a method to produce highly porous and crystalline MIL-100(Fe) from iron(III) nitrate and trimesic acid in a homogeneous DMSO/water solution at ambient pressure as the main advantage over existing MIL-100(Fe) preparations. This facilitates potential industrial production as more expensive pressure vessels and concomitant precautions are not necessary. Further, the MIL product can be collected by simple solid/liquid separation, *e.g.*, by filtration or centrifugation as unreacted trimesic acid remains in solution. Mechanistically, a specific redox pathway is claimed, based on the reaction of DMSO and its decomposition products with redox-active nitrate anions. This claim is strengthened by the negative results of comparative reaction systems using non-redox-active chloride, mesylate or sulfate anions. The overall procedure is especially promising not only for the deposition of coatings, but also for to the industrial production of this MOF, where heterogeneous, hydrothermal (pressure) reaction conditions should be avoided.

Further research should be focused on increasing the reaction yield, solvent regeneration and product extraction. Further research could also be directed to combine the ambient pressure process with *in situ* coating procedures, *e.g.*, the substrate heating method,[12] or the cathodic electrodeposition method.[43a]

Acknowledgements

The work was supported by the Federal German Ministry of Economics (BMWi) under grant-# 0327851A/B and by the Federal German Ministry of Education and Research (BMBF) under grant-# 03SF0492A/C.

Notes and references

1 (*a*) G. Férey, *Dalton Trans.*, 2009, 4400–4415; (*b*) C. Serre, S. Kitagawa and P. D. Dietzel, *Microporous Mesoporous Mater.*, 2012, **157**, 1–2; (*c*) J. R. Long and O. M. Yaghi, *Chem. Soc. Rev.*, 2009, **38**, 1213–1214; (*d*) H. C. Zhou, J. R. Long and O. M. Yaghi, *Chem. Rev.*, 2012, **112**, 673–674; (*e*) C. Janiak and J. K. Vieth, *New J. Chem.*, 2010, **34**, 2366–2388; (*f*) S. H. Jhung, N. A. Khan and Z. Hasan, *CrystEngComm*, 2012, **14**, 7099–7109; (*g*) M. Gaab, N. Trukhan, S. Maurer, R. Gummaraju and U. Müller, *Microporous Mesoporous Mater.*, 2012, **157**, 131–136.

2 G. Férey, *Chem. Soc. Rev.*, 2008, **37**, 191–214.

3 (*a*) J. R. Li, R. J. Kuppler and H. C. Zhou, *Chem. Soc. Rev.*, 2009, **38**, 1477–1504; (*b*) M. P. Suh, H. J. Park, T. K. Prasad and D. W. Lim, *Chem. Rev.*, 2012, **112**, 782–835; (*c*) R. B. Getman, Y.-S. Bae, C. E. Wilmer and R. Q. Snurr, *Chem. Rev.*, 2012, **112**, 703–723; (*d*) H. Wu, Q. Gong, D. H. Olson and J. Li, *Chem. Rev.*, 2012, **112**, 836–868; (*e*) L. Wu, M. Xue, S.-L. Qiu, G. Chaplais, A. Simon-Masseron and J. Patarin, *Microporous Mesoporous Mater.*, 2012, **157**, 75–81; (*f*) L. J. Murray, M. Dincă and J. R. Long, *Chem. Soc. Rev.*, 2009, **38**, 1294–1314; (*g*) Z. Chen, S. Xiang, H. D. Arman, P. Li, S. Tidrow, D. Zhao and B. Chen, *Eur. J. Inorg. Chem.*, 2010, 3745–3749.

4 (*a*) Z. Zhang, Y. Zhao, Q. Gong, Z. Li and J. Li, *Chem. Commun.*, 2013, **49**, 653–661; (*b*) J. R. Li, J. Sculley and H. C. Zhou, *Chem. Rev.*, 2012, **112**, 869–932; (*c*) J.-R. Li, Y. Ma, M. C. McCarthy, J. Sculley, J. Yu, H.-K. Jeong, P. B. Balbuena and H.-C. Zhou, *Coord. Chem. Rev.*, 2011, **255**, 1791–1823; (*d*) B. Zheng, H. Liu, Z. Wang, X. Yu, P. Yi and J. Bai, *CrystEngComm*, 2013, **15**, 3517–3520; (*e*) T.-Z. Zhang, Z.-M. Zhang, Y. Lu, H. Fu and E.-B. Wang, *CrystEngComm*, 2013, **15**, 459–462; (*f*) C. Hou, Q. Liu, T.-A. Okamura, P. Wang and W.-Y. Sun, *CrystEngComm*, 2012, **14**, 8569–8576; (*g*) W.-Y. Gao, Y. Niu, Y. Chen, L. Wojtas, J. Cai, Y.-S. Chen and S. Ma, *CrystEngComm*, 2012, **14**, 6115–6117; (*h*) Z. R. Herm, R. Krishna and J. R. Long, *Microporous Mesoporous Mater.*, 2012, **157**, 94–100; (*i*) M. G. Plaza, A. M. Ribeiro, A. Ferreira, J. C. Santos,

Y. K. Hwang, Y. K. Seo, U. H. Lee, J. S. Chang, J. M. Loureiro and A. E. Rodrigues, *Microporous Mesoporous Mater.*, 2012, **153**, 178–190; (*j*) C. Li, W. Qiu, W. Shi, H. Song, G. Bai, H. He, J. Li and M. J. Zaworotko, *CrystEngComm*, 2012, **14**, 1929–1932; (*k*) H. B. Tanh Jeazet, C. Staudt and C. Janiak, *Dalton Trans.*, 2012, **41**, 14003–14027; (*l*) B. Zornoza, C. Tellez, J. Coronas, J. Gascon and F. Kapteijn, *Microporous Mesoporous Mater.*, 2013, **166**, 67–78; (*m*) G. Dong, H. Li and V. Chen, *J. Mater. Chem. A*, 2013, **1**, 4610–4630; (*n*) B. Seoane, J. Coronas, I. Gascon, M. E. Benavides, O. Karvan, J. Caro, F. Kapteijn and J. Gascon, *Chem. Soc. Rev.*, 2015, **44**, 2421–2454.

5 G. Férey, C. Serre, T. Devic, G. Maurin, H. Jobic, P. L. Llewellyn, G. de Weireld, A. Vimont, M. Daturi and J. S. Chang, *Chem. Soc. Rev.*, 2011, **40**, 550–562.

6 (*a*) E. M. Dias and C. Petit, *J. Mater. Chem. A*, 2015, **3**, 22484–22506; (*b*) A. J. Howarth, Y. Liu, J. T. Hupp and O. K. Farha, *CrystEngComm*, 2015, **17**, 7245–7253; (*c*) K. A. Cychosz, R. Ahmad and A. J. Matzger, *Chem. Sci.*, 2010, **1**, 293–302.

7 K. A. Cychosz and A. J. Matzger, *Langmuir*, 2010, **26**, 17198–17202.

8 (*a*) M. Yoon, R. Srirambalaji and K. Kim, *Chem. Rev.*, 2012, **112**, 1196–1231; (*b*) J. Guo, J. Yang, Y.-Y. Liu and J.-F. Ma, *CrystEngComm*, 2012, **14**, 6609–6617; (*c*) J. Lee, O. K. Farha, J. Roberts, K. A. Scheidt, S. T. Nguyen and J. T. Hupp, *Chem. Soc. Rev.*, 2009, **38**, 1450–1459; (*d*) B. J. Burnett, P. M. Barron and W. Choe, *CrystEngComm*, 2012, **14**, 3839–3846; (*e*) H.-J. Pang, H.-Y. Ma, J. Peng, C.-J. Zhang, P.-P. Zhang and Z.-M. Su, *CrystEngComm*, 2011, **13**, 7079–7085.

9 A. Herbst, A. Khutia and C. Janiak, *Inorg. Chem.*, 2014, **53**, 7319–7333.

10 (*a*) F. Jeremias, D. Fröhlich, C. Janiak and S. K. Henninger, *New J. Chem.*, 2014, **38**, 1846–1852; (*b*) C. Janiak and S. K. Henninger, *Chimia*, 2013, **67**, 419–424; (*c*) C. Janiak and S. K. Henninger, *Nachr. Chem.*, 2013, **61**, 520–523; (*d*) S. K. Henninger, F. Jeremias, H. Kummer and C. Janiak, *Eur. J. Inorg. Chem.*, 2012, 2625–2634; (*e*) S. K. Henninger, H. A. Habib and C. Janiak, *J. Am. Chem. Soc.*, 2009, **131**, 2776–2777; (*f*) J. Ehrenmann, S. K. Henninger and C. Janiak, *Eur. J. Inorg. Chem.*, 2011, 471–474; (*g*) F. Jeremias, V. Lozan, S. Henninger and C. Janiak, *Dalton Trans.*, 2013, **42**, 15967–15973; (*h*) D. Fröhlich, S. K. Henninger and C. Janiak, *Dalton Trans.*, 2014, **43**, 15300–15304.

11 F. Jeremias, A. Khutia, S. K. Henninger and C. Janiak, *J. Mater. Chem.*, 2012, **22**, 10148–10151.

12 F. Jeremias, S. K. Henninger and C. Janiak, *Chem. Commun.*, 2012, **48**, 9708–9710.

13 F. Jeremias, D. Fröhlich, C. Janiak and S. K. Henninger, *RSC Adv.*, 2014, **4**, 24073–24082.

14 (*a*) A. U. Czaja, N. Trukhan and U. Muller, *Chem. Soc. Rev.*, 2009, **38**, 1284–1293; (*b*) M. J. Prakash and M. S. Lah, *Chem. Commun.*, 2009, 3326–3341.

15 K. Brandenburg, *Diamond 3.2, Crystal and Molecular Structure Visualization*, Crystal Impact - K. Brandenburg & H. Putz GbR, Bonn, Germany, 2009.

16 (*a*) G. Férey, *Chem. Mater.*, 2001, **13**, 3084–3098; (*b*) G. Férey, C. Mellot-Draznieks, C. Serre and F. Millange, *Acc. Chem. Res.*, 2005, **38**, 217–225; (*c*) G. Férey and C. Serre, *Chem. Soc. Rev.*, 2009, **38**, 1380–1399.

17 (*a*) J. J. Low, A. I. Benin, P. Jakubczak, J. F. Abrahamian, S. A. Faheem and R. R. Willis, *J. Am. Chem. Soc.*, 2009, **131**, 15834–15842; (*b*) J. Canivet, J. Bonnefoy, C. Daniel, A. Legrand, B. Coasne and D. Farrusseng, *New J. Chem.*, 2014, **38**, 3102–3111; (*c*) J. Canivet, A. Fateeva, Y. Guo, B. Coasne and D. Farrusseng, *Chem. Soc. Rev.*, 2014, **43**, 5594–5617.

18 P. Horcajada, S. Surble, C. Serre, D. Y. Hong, Y. K. Seo, J. S. Chang, J. M. Greneche, I. Margiolaki and G. Férey, *Chem. Commun.*, 2007, 2820–2822.

19 (*a*) C. Volkringer, T. Loiseau, M. Haouas, F. Taulelle, D. Popov, M. Burghammer, C. Riekel, C. Zlotea, F. Cuevas, M. Latroche, D. Phanon, C. Knöfelv, P. L. Llewellyn and G. Férey, *Chem. Mater.*, 2009, **21**, 5783–5791; (*b*) P. L. Llewellyn, S. Bourrelly, C. Serre, A. Vimont, M. Daturi, L. Hamon, G. de Weireld, J. S. Chang, D. Y. Hong, Y. Kyu Hwang, S. Hwa Jhung and G. Férey, *Langmuir*, 2008, **24**, 7245–7250; (*c*) L. Hamon, C. Serre, T. Devic, T. Loiseau, F. Millange, G. Férey and G. de Weireld, *J. Am. Chem. Soc.*, 2009, **131**, 8775–8777; (*d*) A. Vimont, J. M. Goupil, J. C. Lavalley, M. Daturi, S. Surble, C. Serre, F. Millange, G. Férey and N. Audebrand, *J. Am. Chem. Soc.*, 2006, **128**, 3218–3227.

20 F. Zhang, J. Shi, Y. Jin, Y. Fu, Y. Zhong and W. Zhu, *Chem. Eng. J.*, 2015, **259**, 183–190.

21 G. Férey, C. Serre, C. Mellot-Draznieks, F. Millange, S. Surble, J. Dutour and I. Margiolaki, *Angew. Chem., Int. Ed.*, 2004, **43**, 6296–6301.

22 G. Akiyama, R. Matsuda and S. Kitagawa, *Chem. Lett.*, 2010, **39**, 360–361.

23 (*a*) J. S. Lee, S. H. Jhung, J. W. Yoon, Y. K. Hwang and J.-S. Chang, *J. Ind. Eng. Chem.*, 2009, **15**, 674–676; (*b*) L. Kurfiřtová, Y.-K. Seo, Y. K. Hwang, J.-S. Chang and J. Čejka, *Catal. Today*, 2012, **179**, 85–90; (*c*) P. Küsgens, M. Rose, I. Senkovska, H. Fröde, A. Henschel, S. Siegle and S. Kaskel, *Microporous Mesoporous Mater.*, 2009, **120**, 325–330.

24 H. Reinsch and N. Stock, *CrystEngComm*, 2013, **15**, 544.

25 A. Lieb, H. Leclerc, T. Devic, C. Serre, I. Margiolaki, F. Mahjoubi, J. S. Lee, A. Vimont, M. Daturi and J.-S. Chang, *Microporous Mesoporous Mater.*, 2012, **157**, 18–23.

26 C. Volkringer, D. Popov, T. Loiseau, G. Férey, M. Burghammer, C. Riekel, M. Haouas and F. Taulelle, *Chem. Mater.*, 2009, **21**, 5695–5697.

27 P. Horcajada, T. Chalati, C. Serre, B. Gillet, C. Sebrie, T. Baati, J. F. Eubank, D. Heurtaux, P. Clayette, C. Kreuz, J. S. Chang, Y. K. Hwang, V. Marsaud, P. N. Bories, L. Cynober, S. Gil, G. Férey, P. Couvreur and R. Gref, *Nat. Mater.*, 2010, **9**, 172–178.

28 R. Canioni, C. Roch-Marchal, F. Sécheresse, P. Horcajada, C. Serre, M. Hardi-Dan, G. Férey, J.-M. Grenèche, F. Lefebvre, J.-S. Chang, Y.-K. Hwang, O. Lebedev, S. Turner and G. van Tendeloo, *J. Mater. Chem.*, 2011, **21**, 1226–1233.
29 Y.-K. Seo, J. W. Yoon, J. S. Lee, U. H. Lee, Y. K. Hwang, C.-H. Jun, P. Horcajada, C. Serre and J.-S. Chang, *Microporous Mesoporous Mater.*, 2012, **157**, 137–145.
30 J. Shi, S. Hei, H. Liu, Y. Fu, F. Zhang, Y. Zhong and W. Zhu, *J. Chem.*, 2013, **2013**, 1–4.
31 M. Yamashita, M. Yamashita, M. Suzuki, H. Hirai and H. Kajigaya, *Crit. Care Med.*, 2001, **29**, 1575–1578.
32 (*a*) M. Faustini, J. Kim, G.-Y. Jeong, J. Y. Kim, H. R. Moon, W.-S. Ahn and D.-P. Kim, *J. Am. Chem. Soc.*, 2013, **135**, 14619–14626; (*b*) P. A. Bayliss, I. A. Ibarra, E. Pérez, S. Yang, C. C. Tang, M. Poliakoff and M. Schröder, *Green Chem.*, 2014, **16**, 3796; (*c*) M. P. Batten, M. Rubio-Martinez, T. Hadley, K.-C. Carey, K.-S. Lim, A. Polyzos and M. R. Hill, *Curr. Opin. Chem. Eng.*, 2015, **8**, 55–59.
33 S. Waitschat, M. T. Wharmby and N. Stock, *Dalton Trans.*, 2015, **44**, 11235–11240.
34 N. Stock and S. Biswas, *Chem. Rev.*, 2012, **112**, 933–969.
35 T. Zhao, F. Jeremias, I. Boldog, B. Nguyen, S. K. Henninger and C. Janiak, *Dalton Trans.*, 2015, **44**, 16791–16801.
36 Gaylord Chemical, Dimethyl Sulfoxide (DMSO). Physical Properties - Bulletin # 101, http://www.gaylordchemical.com/65-2/literature/101b-dmso-physical-properties/, 2005.
37 H. Dehn, *US Pat*, 3463684, 1969.
38 R. C. Paul, R. C. Narula and S. K. Vasisht, *Transition Met. Chem.*, 1978, **3**, 35–38.
39 E. A. Berdonosova, K. A. Kovalenko, E. V. Polyakova, S. N. Klyamkin and V. P. Fedin, *J. Phys. Chem. C*, 2015, **119**, 13098–13104.
40 (*a*) W. B. Moniz, C. F. Poranski and D. L. Venezky, *U. S. Gov. Res. Dev. Rep.*, 1968, 1–38; (*b*) J. R. Tzou, M. Mullaney, R. E. Norman and S. C. Chang, *Acta Crystallogr., Sect. C: Cryst. Struct. Commun.*, 1995, **51**, 2249–2252.
41 Gaylord Chemical, Dimethyl Sulfide Reaction Solvent Guide - Bulletin # 203B, http://www.gaylordchemical.com/?page=203b-dms-reaction-solvent-guide, 2007.
42 A. Saytzeff, *Liebigs Ann. Chem.*, 1867, **144**, 148–156.
43 (*a*) M. Li and M. Dincă, *J. Am. Chem. Soc.*, 2011, **133**, 12926–12929; (*b*) M. Li and M. Dincă, *Chem. Mater.*, 2015, **27**, 3203–3206.